TANGO1 and Mia2/cTAGE5 (TALI) cooperate to export bulky pre-chylomicrons/VLDLs from the endoplasmic reticulum

António J.M. Santos,[1,2] Cristina Nogueira,[1,2] Maria Ortega-Bellido,[1,2] and Vivek Malhotra[1,2,3]

[1]Centre for Genomic Regulation, The Barcelona Institute of Science and Technology, 08003 Barcelona, Spain
[2]Universitat Pompeu Fabra, 08002 Barcelona, Spain
[3]Institució Catalana de Recerca i Estudis Avançats, 08010 Barcelona, Spain

Procollagens, pre-chylomicrons, and pre–very low-density lipoproteins (pre-VLDLs) are too big to fit into conventional COPII-coated vesicles, so how are these bulky cargoes exported from the endoplasmic reticulum (ER)? We have shown that TANGO1 located at the ER exit site is necessary for procollagen export. We report a role for TANGO1 and TANGO1-like (TALI), a chimeric protein resulting from fusion of MIA2 and cTAGE5 gene products, in the export of pre-chylomicrons and pre-VLDLs from the ER. TANGO1 binds TALI, and both interact with apolipoprotein B (ApoB) and are necessary for the recruitment of ApoB-containing lipid particles to ER exit sites for their subsequent export. Although export of ApoB requires the function of both TANGO1 and TALI, the export of procollagen XII by the same cells requires only TANGO1. These findings reveal a general role for TANGO1 in the export of bulky cargoes from the ER and identify a specific requirement for TALI in assisting TANGO1 to export bulky lipid particles.

Introduction

The majority of secretory proteins are known to be exported from the ER by COPII-coated vesicles (Lord et al., 2013). These COPII carriers are formed at ER exit sites upon activation of the small GTPase Sar1 by a protein called Sec12 (Nakańo and Muramatsu, 1989; Barlowe and Schekman, 1993). The activation of Sar1 leads to recruitment of the inner-coat proteins Sec23/24 followed by attachment of the outer-coat proteins Sec13/31 and GTP hydrolysis to generate a small coated vesicle of 60- to 90-nm diameter (Kuehn et al., 1998; Matsuoka et al., 1998; Stagg et al., 2006). However, several secreted cargoes, including procollagens, pre-chylomicrons, and large pre–very low-density lipoproteins (pre-VLDLs), are too big to fit into these vesicles (Fromme and Schekman, 2005; Malhotra and Erlmann, 2011; Malhotra et al., 2015). How are these bulky cargoes exported from the ER?

The identification of TANGO1 as a transmembrane receptor for procollagen VII at ER exit sites (Saito et al., 2009) has begun to shed light on the mechanism by which big cargoes exit the ER. The binding of TANGO1 to procollagen VII in the lumen of the ER requires TANGO1's SH3-like domain. The proline-rich domain of TANGO1 interacts with COPII-coat components Sec23/24 on the cytoplasmic side of the ER (Saito et al., 2009, 2011). TANGO1's TEER domain (a coiled-coil–containing region from residues 1,214–1,396 aa) recruits ER–Golgi intermediate compartment (ERGIC) membranes to procollagen-enriched domains at the ER followed by their subsequent fusion to generate an export pathway for procollagens (Santos et al., 2015). The second coiled-coil domain of TANGO1 binds a protein called cTAGE5 on the cytoplasmic side of the ER (Saito et al., 2011). cTAGE5, unlike TANGO1, lacks a lumenal domain and therefore cannot bind to cargoes. Nonetheless, the first coiled-coil domain of cTAGE5 binds and recruits Sec12, which likely increases the recruitment of the inner COPII-coat proteins Sec23/24. The increase in the amount of outer-coat proteins Sec13/31 commensurate with the increased pool of Sec23/24 could be mediated by the ubiquitination of Sec31 by the ubiquitin ligase KLHL12 (Jin et al., 2012). In addition, a protein called Sedlin has been proposed to modulate the size of nascent vesicles by regulating Sar1-mediated COPII-coat dynamics (Venditti et al., 2012). Altogether, the functions of TANGO1, cTAGE5, KLHL12, and Sedlin provide a means for cells to export bulky procollagens from the ER (Malhotra and Erlmann, 2015; Malhotra et al., 2015).

But how are bulky lipid particles such as pre-chylomicrons and pre-VLDLs exported from the ER? Chylomicrons and large VLDLs are big particles of ∼150–500 nm and up to 90-nm diameter, respectively, that are mainly composed of

Correspondence to Vivek Malhotra: vivek.malhotra@crg.eu

Abbreviations used in this paper: Apo, apolipoprotein; BFA, Brefeldin A; CRISPR, clustered regularly interspaced short palindromic repeat; ERGIC, ER–Golgi intermediate compartment; gRNA, guide RNA; KO, knockout; MTP, microsomal triglyceride transfer protein; PDI, protein disulfide isomerase; VLDL, very low-density lipoprotein.

The Rockefeller University Press $30.00
J. Cell Biol. Vol. 213 No. 3 343–354
www.jcb.org/cgi/doi/10.1083/jcb.201603072

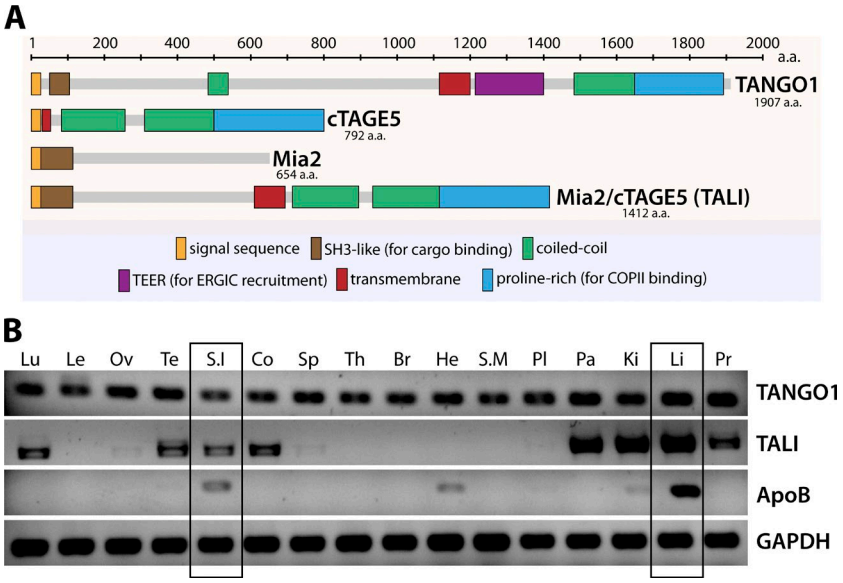

Figure 1. **Chimeric Mia2/cTAGE5 (TALI) is structurally similar to TANGO1 and is expressed in the small intestine and liver, together with TANGO1 and ApoB.** (A) Scheme depicting the domains of full-length TANGO1, cTAGE5, Mia2, and TALI. Each domain corresponds to the stretch of amino acid sequence represented by the numbers above it. (B) cDNAs from different human tissues screened for expression of TANGO1, TALI, ApoB, or the housekeeping gene GAPDH. Lu, lung; Le, leukocyte; Ov, ovary; Te, testis; S.I, small intestine; Co, colon; Sp, spleen; Th, thymus; Br, brain; He, heart; S.M, skeletal muscle; Pl, placenta; Pa, pancreas; Ki, kidney; Li, liver; Pr, prostate. The rows corresponding to the small intestine and liver profiles are highlighted; $n = 3$.

triglycerides, but also contain phospholipids and cholesterol (Ruf and Gould, 1999; Zheng et al., 2006; Nakajima et al., 2014). The lipid core of these particles is decorated with apolipoprotein B (ApoB). Assembly of pre-chylomicrons and pre-VLDLs at the ER is regulated by a chaperone called microsomal triglyceride transfer protein (MTP), which initiates the incorporation of ApoB into lipids and plays a role in ApoB folding and stability (Jiang et al., 2008; Iqbal and Hussain, 2009). These lipid particles are secreted by cells of the liver and small intestine, and a defect in their export impairs the homeostasis of cholesterol and triglycerides.

A fusion transcript composed of exons from *cTAGE5* and exons from its immediate distal gene *MIA2* was identified in mice (Pitman et al., 2011). Because cTAGE5 and the cytosolic part of TANGO1 contain homologous domains that are organized in the same order; and because MIA2 has an SH3-like domain, the resulting chimeric cTAGE5/MIA2 is a novel protein that exhibits extensive structural homology with TANGO1 (Fig. 1 A; Pitman et al., 2011). Like TANGO1, chimeric cTAGE5/MIA2 localizes to ER exit sites, and a mutation in its SH3-like domain has been found to correlate with a systemic reduction in the plasma levels of cholesterol and triglycerides in mice, indicating a possible role for this ER protein in the metabolism of cholesterol (Pitman et al., 2011). In addition, many genome-wide association studies have shown that the single-nucleotide polymorphism rs17465637, located on chromosome 1q41 in an intronic region of *TANGO1*, confers increased risk of coronary artery disease and atherosclerosis (Roder et al., 2011; García-Bermúdez et al., 2012; Li et al., 2013). Several studies have identified circulating chylomicrons and VLDLs as a major contributor to the accumulation of atherosclerotic plaque. Therefore, an association between their secretion and clearance and the development of atherosclerosis, although mechanistically not clear, is currently well accepted (Pal et al., 2003; Proctor and Mamo, 2003; Nakano et al., 2008; Tomkin and Owens, 2012).

Because there is no known receptor for the exit of bulky ApoB-containing particles, such as pre-chylomicrons and pre-VLDLs, we tested whether their export from the ER required TANGO1 and chimeric cTAGE5/MIA2, which we named TALI (for TANGO1-like). Our data show that loss of TANGO1 or TALI in intestinal Caco-2 (human epithelial colorectal adenocarcinoma) and liver HepG2 (human hepatocellular carcinoma) cells, which produce and secrete chylomicrons and VLDLs, respectively (van Greevenbroek et al., 2000; Meex et al., 2011; Jammart et al., 2013; Nauli et al., 2014), reduces ApoB secretion. We further show that TANGO1 interacts with TALI, and both interact with ApoB, to recruit bulky lipid particles to ER exit sites. Loss of either TANGO1 or TALI leads to an accumulation of ApoB in the ER that is eventually subjected to autophagy.

Results

TALI is a novel human protein that is structurally similar to TANGO1

A fusion transcript composed of exons from *cTAGE5* and exons from *MIA2* was previously identified in mice (Pitman et al., 2011). Because the resulting protein is structurally similar to TANGO1, we first assessed whether such a transcript also occurs in humans. We started by extracting total RNA from Caco-2 cells and then produced cDNA by RT-PCR. With primers complementary to the initial N-terminal region of *MIA2* and to the end of the C-terminal region of *cTAGE5*, we obtained a DNA fragment that, upon sequencing, was revealed to correspond to a fusion of the Ensembl-annotated transcripts MIA2-001 and cTAGE5-001 (Yates et al., 2016). This fusion protein, henceforth referred to as TALI, carries the signal sequence from MIA2 but not of cTAGE5, because its transcript does not include exon 1 from the latter. Importantly, the transcript we identified for TALI contains exon 5 from *MIA2*, which is not the case for the only Ensembl-annotated MIA2/cTAGE5 fusion transcript RP11-407N17.3-001 (ENST00000553728) in humans (Yates et al., 2016). Interestingly, computational analysis of the sequence of *TALI* (unpublished data) revealed that, in addition to the transmembrane domain of *cTAGE5*, the fusion between exon 6 of *MIA2* and exon 2 of *cTAGE5* generates a second membrane-insertion sequence, which results in a transmembrane portion that is remarkably similar to the transmembrane regions of *TANGO1* (Fig. 1 A). Pitman et al. (2011) reported that a mutation in the SH3-like domain of the mouse orthologue MIA2/cTAGE5 chimera caused a reduction in cholesterol and

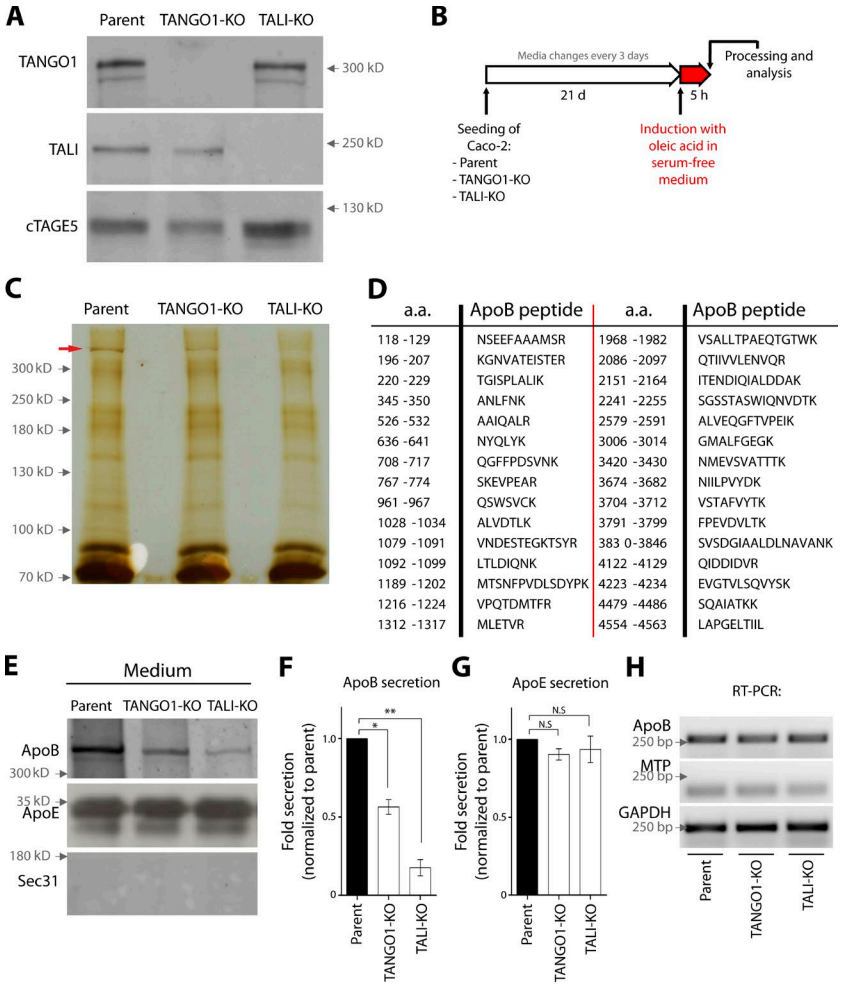

Figure 2. **Knockout of TANGO1 or TALI impairs secretion of ApoB-containing lipid particles.** (A) Western blot of differentiated parental and TANGO1- and TALI-CRISPR KO Caco-2 cells (TANGO1-KO and TALI-KO). Protein lysates were separated on a 6% SDS-PAGE, transferred onto a nitrocellulose membrane, and probed by Western blotting with anti-TANGO1 or anti-cTAGE5 antibodies; $n = 3$. (B) Scheme depicting the methodology used to differentiate and induce chylomicron secretion in Caco-2 cells. (C) Silver-stained gel showing proteins secreted by parental, TANGO1-KO, and TALI-KO differentiated Caco-2 cells after induction. The red arrow points to the band excised and subjected to mass spectrometry analysis; $n = 3$. (D) Sequences of the 30 unique peptides corresponding to ApoB as a result of mass spectrometry analysis. (E) ApoB and apoE secretion was measured by Western blotting probing supernatants collected after 5 h of induction with FCS-free medium with oleic acid. Intensities of signal in the supernatant were recorded by densitometry. Sec31 was used as a lysis control; $n = 6$. (F and G) Secreted ApoB and apoE levels were measured by densitometry quantification and normalized to parental cells; error bars: SEM. *, $P < 0.05$; **, $P < 0.01$; N.S, not statistically significant. (H) Total RNA was extracted from differentiated parental, TANGO1-KO, or TALI-KO Caco-2 cells, and cDNA was produced by RT-PCR and amplified to assess expression of ApoB, MTP, or the housekeeping gene GAPDH; $n = 3$.

triglyceride levels in the plasma of mice. Because TANGO1 is required for bulky procollagen export from the ER and has been associated with cardiovascular disease, and because a mutation in the mouse orthologue of TALI impairs cholesterol homeostasis, we hypothesized that TANGO1 and/or TALI is required for the export of bulky ApoB-containing particles from the ER.

We first screened a panel of cDNAs from 16 human tissues to assess the expression profiles of TANGO1, TALI, and ApoB. Although expression of TANGO1 was apparent in all tissues tested, the expression of TALI was specific to lung, testis, small intestine, colon, pancreas, kidney, liver, and prostate (Fig. 1 B). Interestingly, both TANGO1 and TALI are expressed in small intestine and liver, the tissues that produce and secrete ApoB-containing chylomicrons and VLDLs, respectively (Fig. 1 B).

TANGO1 and TALI are required for secretion of ApoB-containing lipid particles

We next tested whether TANGO1 and TALI were required for secretion of ApoB, a protein that forms the shell of chylomicrons and VLDLs. We generated Caco-2 cell lines in which endogenous TANGO1 and TALI were deleted by the clustered regularly interspaced short palindromic repeat (CRISPR)/Cas9 system (Cong et al., 2013; Mali et al., 2013). Western blots confirmed the complete absence of TANGO1 and TALI in Caco-2 cells by the CRISPR/Cas9 method. Importantly, the TALI guide RNAs (gRNAs) were designed to target the sequence corresponding to *MIA2*, and so cTAGE5 expression was not affected (Fig. 2 A). Although Caco-2 cells are derived from a colon carcinoma, upon polarization they are morphologically and functionally similar to the enterocytes of the small intestine and thus a well-established system to study the form and function of enterocytes. To induce the secretion of chylomicrons, we seeded parental and CRISPR-cells (TANGO1-knockout [KO] and TALI-KO), and allowed them to differentiate for 21 d. At that time, the cells were washed and incubated with fresh FCS-free medium containing oleic acid (1.5 mM; Fig. 2 B). After 5 h, we collected the medium and, after TCA precipitation, visualized secreted proteins on a 6% SDS-PAGE gel by silver staining. A protein corresponding to a size greater than 300 kD was present in the medium of parental cells but was substantially reduced in the medium of both TANGO1-KO and TALI-KO cells (Fig. 2 C). The band from the parental sample was excised from the gel and identified by mass spectrometric analysis. This procedure revealed 30 peptides that were specific for ApoB (Fig. 2 D), which indicated a role for TANGO1 and TALI in the secretion of ApoB-containing particles. To confirm the results obtained by mass spectrometry, we repeated the secretion-inducing procedure described earlier, but this time we probed the supernatants of parental, TANGO1-KO, and TALI-KO cells by Western blotting with an anti-ApoB antibody. As expected, knockout of TANGO1 and TALI led to a block in secretion of ApoB to ∼44% and 82%, respectively, compared with the parental cells (Fig. 2, E and F). On the other hand, secretion of apoE, a lipoprotein that associates with chylomicrons

extracellularly and does not play a role in their assembly or secretion (Plump et al., 1992; Zhang et al., 1992), was not affected in the TANGO1 and TALI KO cells (Fig. 2, E and G). To test whether the reduction in secretion of ApoB in the absence of TANGO1 or TALI was caused by down-regulation of the mRNA levels of ApoB or MTP, a chaperone that is necessary for the folding and assembly of ApoB-containing lipid particles at the ER, we extracted total RNA from differentiated parental, TANGO1-KO, and TALI-KO Caco-2 cells and produced cDNA by RT-PCR. We did not detect any differences in the levels of mRNA of ApoB or MTP between the parental and KO cells (Fig. 2 H). Altogether, these findings indicate that secretion of fully assembled chylomicrons is impaired in the absence of TANGO1 or TALI.

Export from the ER of ApoB-containing lipid particles is impaired in cells deleted of TANGO1 or TALI

We then assessed the intracellular fate of ApoB in TANGO1-KO and TALI-KO cells. The differentiated Caco-2 cells were treated with oleic acid for 5 h, as before (Fig. 2 B), and then fixed and immunostained for ApoB and ER markers. Immunofluorescence microscopy revealed, to our surprise, no detectable accumulation of ApoB in the ER of TANGO1-KO or TALI-KO cells. Because an autophagy-mediated pathway has been described previously as a means to degrade excessive intracellular ApoB (Brodsky and Fisher, 2008; Olofsson and Borén, 2012), we tested whether this was the case upon KO of TANGO1 or TALI. Indeed, absence of either TANGO1 or TALI led to an intracellular accumulation of ApoB that significantly colocalized with LAMP1, in contrast with parental cells (Fig. 3 A). Because LAMP1 is a lysosomal protein and also a marker of autolysosomes, derived from the fusion of an autophagosome and a lysosome (Korolchuk et al., 2011), we next immunostained the cells for LC3, a marker of autophagosomes (Xie and Klionsky, 2007). Indeed, ApoB accumulations in TANGO1-KO or TALI-KO cells also significantly colocalized with LC3, unlike parental cells (Fig. 3 B). Because TANGO1 and TALI are transmembrane proteins at the ER, we hypothesized that the intracellular accumulation of ApoB in the KO cells started as an arrest at the ER that was followed by targeting into LAMP1- and LC3-positive compartments as a result of autophagy (Bernales et al., 2007; Khaminets et al., 2015). Thus, inhibiting the formation of autophagosomes would lead to an arrest of ApoB in the ER in the KO cells, but not in parental cells. To test this, we treated differentiated Caco-2 cells with wortmannin, an inhibitor of phosphatidylinositol 3-kinase and thus autophagy (Blommaart et al., 1997), in addition to oleic acid (Fig. 4 A). We first tested whether wortmannin had an effect on the secretion of ApoB by Western blotting of the supernatants of parental, TANGO1-KO, and TALI-KO Caco-2 cells with or without wortmannin treatment (method in Fig. 2 B compared with Fig. 4 A). We did not detect significant differences in secreted ApoB as a result of wortmannin treatment (Fig. 4, B and C). This rules out the possibility of an autophagy-mediated export of ApoB from the ER. Next, immunofluorescence microscopy confirmed that upon autophagy inhibition, TANGO1-KO and TALI-KO cells showed a significant accumulation of ApoB that colocalized with the ER marker protein disulfide isomerase (PDI), in contrast to parental cells (Manders coefficient ~0.62 for TANGO1-KO and ~0.80 for TALI-KO, compared with ~0.30 in parental cells; Fig. 4, D and E). In agreement with our data from the secretion assays (Fig. 2, E and G), we did not detect any intracellular accumulations of apoE by immunofluorescence microscopy (Fig. 4 F). Because Caco-2 cells mainly assemble and secrete chylomicrons, but large VLDLs are also ApoB-containing lipid particles reported to leave the ER in vesicles bigger than COPII-coated vesicles (100–120 nm compared with 60–90 nm; Siddiqi, 2008), we tested whether the absence of TANGO1 or TALI also led to an intracellular accumulation of ApoB in HepG2 cells, a liver cell line commonly used to study VLDL assembly and secretion (Meex et al., 2011). After generating HepG2 cell lines in which endogenous TANGO1 and TALI were knocked out by the CRISPR/Cas9 system (not depicted), we first let the HepG2 cells grow for 5–10 d, then

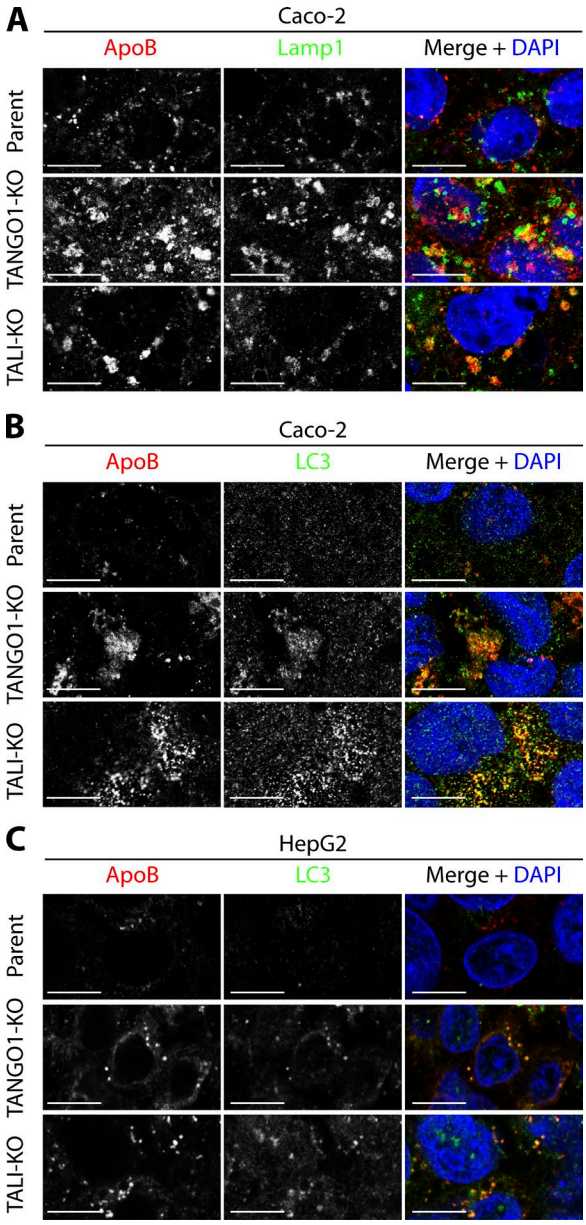

Figure 3. **ApoB is targeted by autophagy in the absence of TANGO1 or TALI.** (A and B) Differentiated parental, TANGO1-KO, or TALI-KO Caco-2 cells, induced for secretion of chylomicrons, were fixed with methanol and immunostained for ApoB (red) and LAMP1 or LC3 (green). DAPI is shown in blue. (C) Parental, TANGO1-KO, or TALI-KO HepG2 cells, induced for secretion of VLDLs, were fixed with methanol and immunostained for ApoB (red) and LC3 (green). DAPI is shown in blue. Bars, 10 µm. *n* = 4.

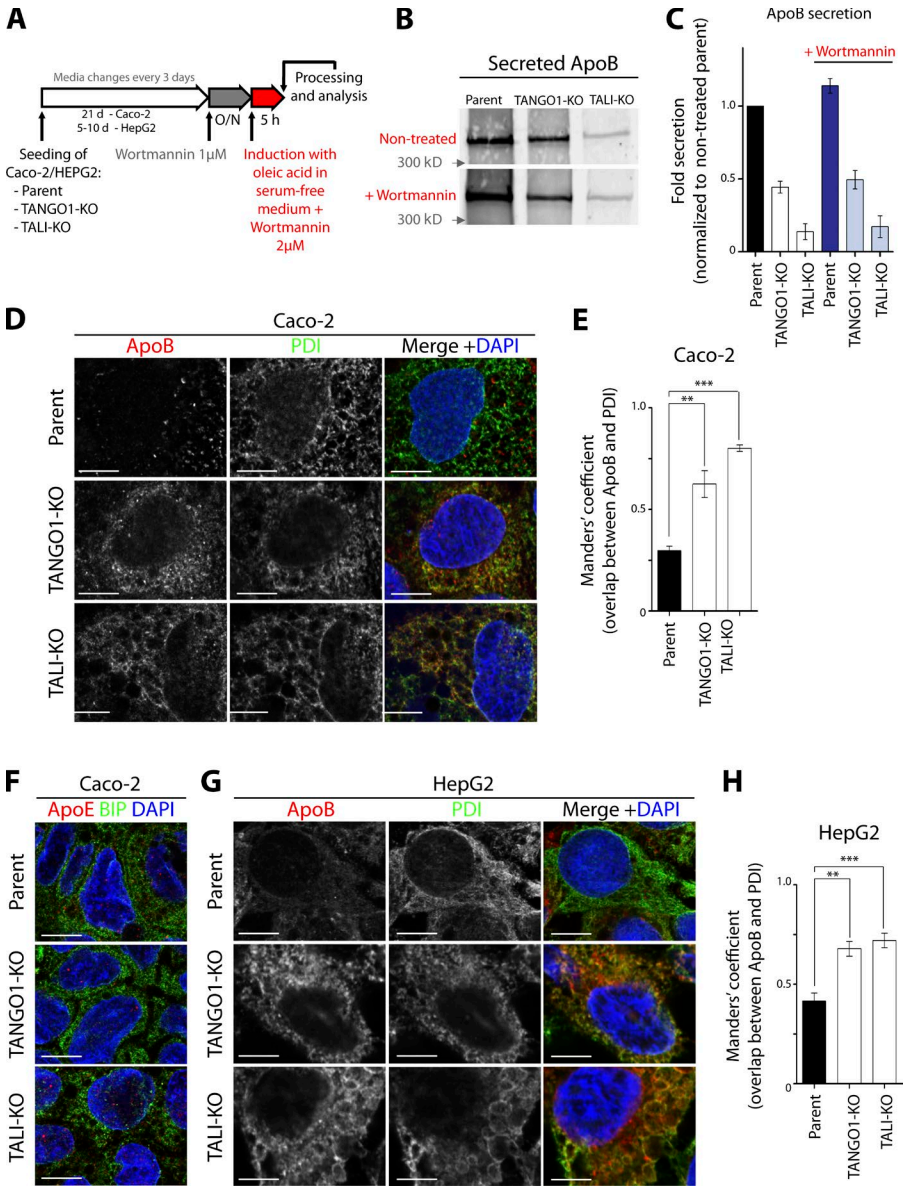

Figure 4. **KO of TANGO or TALI blocks pre-chylomicrons and pre-VLDLs at the ER upon treatment with wortmannin.** (A) Scheme depicting the methodology used to differentiate and induce chylomicron or VLDL secretion in Caco-2 or HepG2 cells, respectively, while inhibiting autophagy. (B) ApoB secretion was assessed by Western blot by probing supernatants collected after 5 h of incubation with FCS-free medium containing oleic acid in the presence or absence of the autophagy inhibitor wortmannin; intensities of signal in the supernatant were recorded by densitometry. $n = 3$. (C) Secreted ApoB levels with or without the autophagy inhibitor wortmannin were measured by densitometry quantification. Error bars: SEM; $n = 3$. (D) Differentiated parental, TANGO1-KO, or TALI-KO Caco-2 cells, induced for secretion of chylomicrons with autophagy inhibition by wortmannin, were fixed with methanol and immunostained for ApoB (red) and PDI (green). DAPI is shown in blue. Bars, 10 µm. (E) Colocalization quantifications were calculated by Manders correlation coefficient by measuring the overlap between the green and the red channels. Error bars: SEM; **, $P < 0.01$; ***, $P < 0.001$; ≥100 cells per experiment; $n = 3$. (F) Differentiated parental, TANGO1-KO, or TALI-KO Caco-2 cells, induced for secretion of chylomicrons with autophagy inhibition by wortmannin, were fixed with methanol and immunostained for apoE (red) and BIP (green). DAPI is shown in blue. Bars, 10 µm. (G) Parental, TANGO1-KO, or TALI-KO HepG2 cells, induced for secretion of VLDLs with autophagy inhibition by wortmannin, were fixed with methanol and immunostained for ApoB (red) and PDI (green). DAPI is shown in blue. Bars, 10 µm. (H) Colocalization quantifications were calculated by Manders correlation coefficient by measuring the overlap between the green and the red channels. Error bars: SEM; **, $P < 0.01$; ***, $P < 0.001$; ≥100 cells per experiment; $n = 3$.

subjected them to wortmannin treatment, to inhibit autophagy, and oleic acid, to induce VLDL secretion (Fig. 4 A). Similar to what we observed in Caco-2 cells, immunofluorescence microscopy confirmed that upon autophagy inhibition, TANGO1-KO and TALI-KO cells showed a significant accumulation of ApoB that colocalized with the ER marker PDI, in contrast to parental cells (Manders coefficient ∼0.68 for TANGO1-KO and ∼0.72 for TALI-KO, compared with ∼0.42 in parental cells; Fig. 4, G and H). In agreement with our observation in Caco-2 cells, without wortmannin treatment, the absence of TANGO1 and TALI in HepG2 cells led to intracellular accumulations of ApoB in LC3-positive compartments (Fig. 3 C). Altogether, these data indicate that the absence of TANGO1 or TALI leads to an arrest of ApoB in the ER that is subjected to autophagy.

Knockout of TANGO1, but not of TALI, blocks export of collagen XII from the ER

Because TANGO1 is known for its role in exporting procollagens from the ER, we tested whether loss of TANGO1 and TALI affected collagen secretion in differentiated Caco-2 cells in FCS-free medium with ascorbic acid for 20 h (Fig. 5 A). Media and the cell lysates of cells deleted of TANGO1 or TALI were analyzed by Western blotting. This approach revealed that KO of TANGO1, but not of TALI, resulted in an accumulation of intracellular collagen XII and a considerable reduction in its secreted levels (Fig. 5, B and C). To assess in which cellular compartment collagen XII was arrested in the absence of TANGO1, we stained cells for collagen XII and the ER resident protein PDI. Immunofluorescence analysis showed that collagen XII was arrested at the ER only in the absence of TANGO1, but not in parental cells or TALI-KO cells (Fig. 5 D). These experiments show that although TANGO1 and TALI cooperate to export pre-chylomicrons and pre-VLDLs from the ER, TALI does not participate in the TANGO1-mediated export of procollagen XII from the ER.

TANGO1 and TALI interact with each other and with ApoB at ER exit sites

TANGO1 has been shown to colocalize and interact with cTAGE5 at ER exit sites (Saito et al., 2011). To test whether TALI also colocalized with TANGO1, we generated a construct

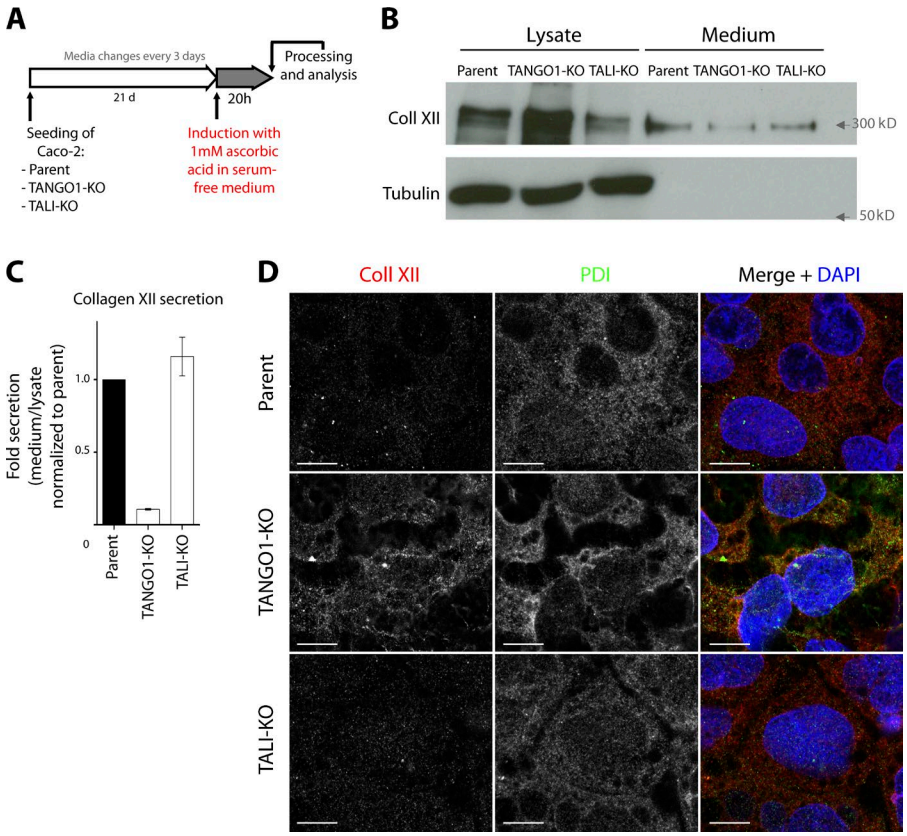

Figure 5. **KO of TANGO, but not TALI, blocks procollagen XII export from the ER.** (A) Scheme depicting the methodology used to differentiate Caco-2 cells and induce secretion of collagens. (B) Lysates and supernatants of differentiated parental, TANGO1-KO, or TALI-KO Caco-2 cells, induced with ascorbic acid for 20 h, underwent Western blotting for collagen XII. Intensities of signal in the supernatant were recorded by densitometry. (C) Ratio of external versus internal collagen XII normalized to parental cells. Error bars: SEM. (D) Differentiated parental, TANGO1-KO, or TALI-KO Caco-2 cells, induced with ascorbic acid for 20 h, were fixed with methanol and immunostained for collagen XII (red) and PDI (green). DAPI is shown in blue. Bars, 10 µm. $n = 3$.

in which an EGFP tag was cloned at the C terminus of TALI and used lentivirus to express the TALI-EGFP fusion protein in Caco-2 cells or transfected it in HepG2 cells. To visualize the intracellular localization of TALI, fixed cells were immunostained for EGFP and TANGO1. Immunofluorescence microscopy revealed that TALI-EGFP colocalized with TANGO1 at ER exit sites in both cell lines (Fig. 6 A), similarly to that reported previously in mouse cells (Pitman et al., 2011). We then tested whether they interacted with each other. HepG2 cells induced with oleic acid for 5 h for VLDL assembly and secretion were lysed, and the cell lysates were immunoprecipitated with anti-TANGO1 or anti-MIA2 antibody. Western blots of the precipitates revealed that TANGO1 and TALI coimmunoprecipitated (Fig. 6 B), indicating they interact with each other at ER exit sites. Because TANGO1 and TALI localize at ER exit sites and the abrogation of either of them by CRI SPR prevents export of ApoB-containing lipid particles from the ER and their subsequent secretion (Figs. 2, 3, and 4), we hypothesized that they also formed a complex with ApoB at ER exit sites. To test this, we used differentiated Caco-2 cells, induced with oleic acid as before (Fig. 2 B), and immunostained for TANGO1 and TALI, using an anti-cTAGE5 antibody for the latter. By immunofluorescence microscopy, we observed that ApoB frequently colocalized with TANGO1 and cTAGE5 at ER exit sites (Fig. 6 C). To test whether they also physically interact with ApoB, HepG2 cells induced with oleic acid for 5 h were lysed, and the cell lysates were immunoprecipitated with anti-TANGO1, anti-cTAGE5, or anti-MIA2 antibody. Western blots of the precipitates against ApoB revealed that all antibodies coimmunoprecipitated ApoB (Fig. 6 D). Importantly, this was the case for both MIA2 and cTAGE5 antibodies (which recognize the lumenal and cytoplasmic sides of TALI, respectively), strongly indicating that, besides TANGO1, the full-length protein TALI physically interacts with ApoB. Altogether, these data strongly indicate that TANGO1 and TALI are in a complex that also contains ApoB.

TANGO1 and TALI cooperate to recruit ApoB-containing lipid particles to ER exit sites

Previous studies have shown that lipidated bulky ApoB-containing lipid particles in the lumen of the ER accumulate in a crescent shape around lipid droplets as they are targeted to the proteasome. This is thought to down-regulate secretion of ApoB-containing lipid particles when they are produced excessively (Ohsaki et al., 2006, 2008). Interestingly, the same authors showed that these crescent-shaped accumulations of ApoB around lipid droplets also occur when export from the ER is inhibited by Brefeldin A (BFA; Ohsaki et al., 2013). We then tested whether the ApoB crescents induced upon BFA treatment colocalized with the ER exit marker Sec31. Differentiated parental Caco-2 cells were incubated with oleic acid and BFA for 5 h (Fig. 7 A). Immunofluorescence microscopy analysis revealed colocalization of the ApoB crescents with Sec31 around lipid droplets, marked with boron-dipyrromethene (BODIPY). This strongly indicates that the BFA treatment arrests fully assembled ApoB-containing particles in the vicinity of ER exit sites (Fig. 7 B, top). Following the same procedure, we also tested the presence of TANGO1 near these ApoB crescents. By immunofluorescence microscopy, staining for TANGO1 was visualized at the ApoB crescents around lipid droplets, which further implies its role in the export of ApoB from the ER and confirms that the crescent-shaped ApoB structures result from an arrest at ER exit sites upon BFA treatment (Fig. 7 B,

middle). We have shown previously that the TEER domain of TANGO1 recruits ERGIC-53–containing membranes to sites of procollagen export from the ER. We have postulated that these ERGIC membranes are necessary for the growth of a mega carrier to accommodate bulky procollagens (Santos et al., 2015). Interestingly, a previous study showed that pre-chylomicron-containing vesicles exiting the ER contain ERGIC-53 (Siddiqi et al., 2003). In agreement, upon fixation and immunostaining the cells for ERGIC-53, we also observed colocalization of ERGIC-53 and the ApoB crescents (Fig. 7 B, bottom), suggesting that ERGIC-53–containing membranes recruited by TANGO1 are also required for the growth of a mega carrier for export of bulky ApoB-containing particles from the ER. Next we tested the effect of BFA treatment in the formation of ApoB crescents in the TANGO1-KO and TALI-KO cells. As before, differentiated Caco-2 cells, with or without wortmannin treatment to inhibit autophagy, were incubated with oleic acid and BFA for 5 h (Fig. 7, A and C). We fixed and immunostained the cells to visualize ApoB, Sec31, and lipid droplets. This approach revealed significant colocalization of ApoB with Sec31 in the parental cells, but not in TANGO1-KO or TALI-KO cells (Manders coefficient ∼0.13–0.18 for TANGO1-KO and TALI-KO, compared with ∼0.43–0.45 for parental cells; Fig. 7, D and E). We also observed a >10-fold increase in the frequency of ApoB crescents in parental cells, but there was no significant increase in ApoB crescents in either TANGO1-KO or TALI-KO cells upon treatment with BFA, with or without wortmannin (Fig. 7 F), which suggests that both TANGO1 and TALI are required to recruit ApoB-containing particles to ER exit sites, indicating that they work as receptors for these bulky cargoes.

Discussion

The process of export of bulky secretory cargoes from the ER

COPII-coated vesicles of 60- to 90-nm diameter export secretory cargoes from the ER but are too small for bulky cargoes such as procollagens or pre-chylomicrons. Collagens are the most abundant of the secretory proteins, as they constitute ∼25% of our dry body weight and are essential for tissue organization and function. ApoB-containing chylomicrons and VLDLs are essential for the homeostasis of circulating triglycerides and cholesterol. So, how are these bulky cargoes exported from the ER and then across the secretory pathway? To address this issue, we need to address three key points: (a) a mechanism to collect cargo in the ER lumen and connect it to the cytoplasmic COPII machinery; (b) a mechanism to increase the membranes needed to encapsulate the bulky cargoes; and (c) a mechanism to increase the size of the COPII coats. TANGO1 appears pivotal in controlling these three processes: TANGO1 at the ER exit sites interacts with procollagens in the lumen and engages with COPII machinery via its cytoplasmic proline-rich domain, and its TEER domain recruits ERGIC membranes, which is necessary for procollagen export (Saito et al., 2009; Santos et al., 2015). This indicates a potential mechanism for accretion of membranes needed to generate a mega–export carrier. The large amounts of COPII coats necessary for the events that ultimately pinch off procollagen-containing domains formed from the fusion of ERGIC membranes to the ER is likely to be accomplished by the functions of cTAGE5. TANGO1 binds cTAGE5, and cTAGE5 recruits Sec12, which in turn brings Sec23/sec24 to the ER exit site. This

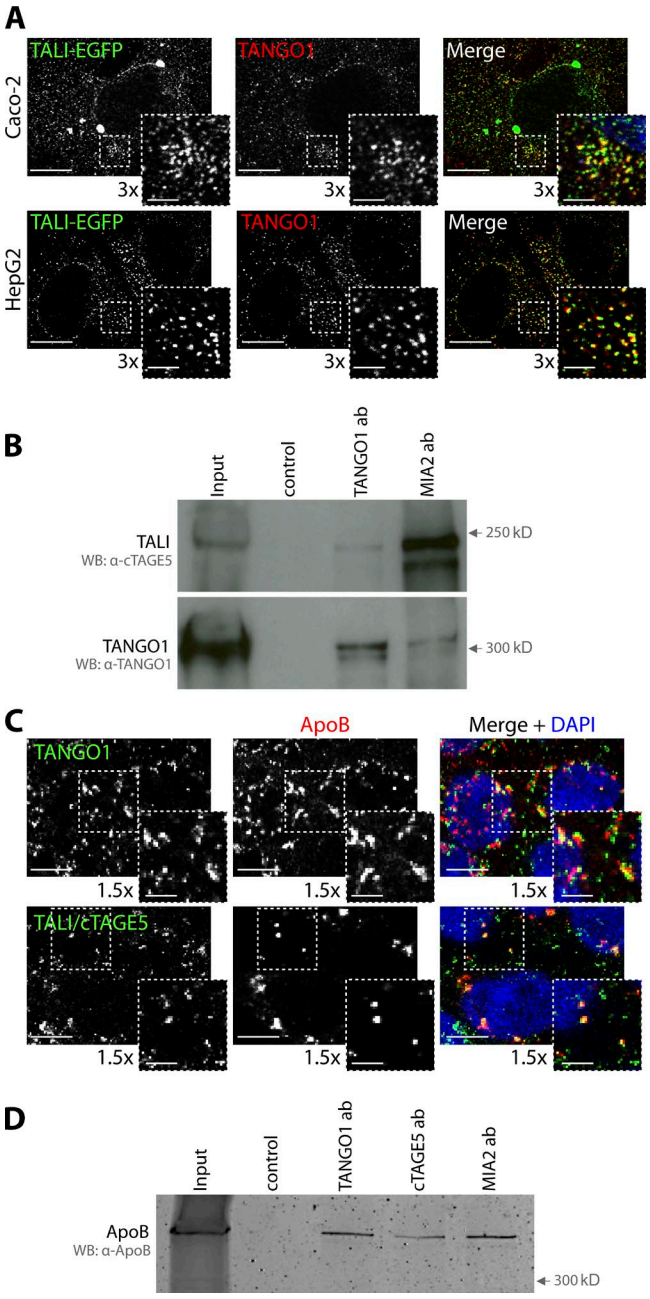

Figure 6. **TANGO1 and TALI form a complex with ApoB at ER exit sites.** (A) Caco-2 cells infected with lentivirus carrying TALI-EGFP or HepG2 transfected with TALI-EGFP were fixed with methanol and immunostained for EGFP (green) and TANGO1 (red). Bars: 10 µm; (boxes) 2.5 µm. (B) Lysates from HepG2 cells induced for VLDL secretion were incubated with no antibody (Ab; control) or with anti-TANGO1 or anti-MIA2 antibodies and then with protein A–Sepharose beads. Precipitates underwent Western blotting (WB) for TANGO1 and cTAGE5. The input sample corresponded to 10% of the total used for the immunoprecipitation. (C) Differentiated Caco-2 cells, induced for secretion of chylomicrons, were fixed with methanol and immunostained for ApoB (red) and TANGO1 or TALI/cTAGE5 (green). DAPI is shown in blue. Bars: 10 µm; (boxes) 1.25 µm. (D) Lysates from HepG2 cells induced for VLDL secretion were incubated with no antibody (control) or with anti-TANGO1, anti-cTAGE5, or anti-MIA2 antibodies and then with protein A–Sepharose beads. Precipitates underwent Western blotting for ApoB. The input sample corresponded to 10% of the total used for the immunoprecipitation. *n* = 3.

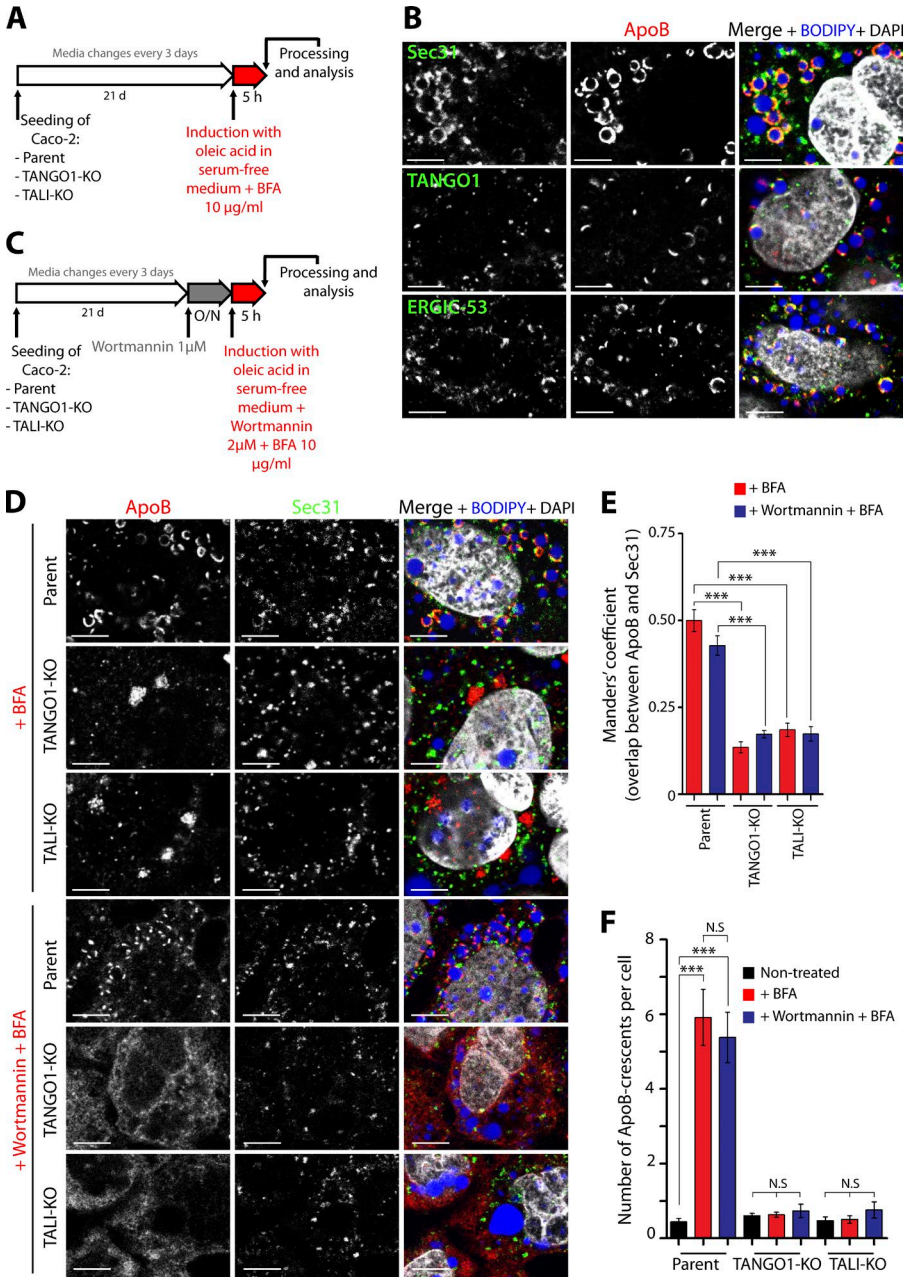

Figure 7. **TANGO1 and TALI are both required for recruitment of ApoB to ER exit sites.** (A) Scheme depicting the methodology used to differentiate and induce chylomicron secretion in Caco-2 while inhibiting ER export with BFA. (B) Differentiated Caco-2 cells, induced for secretion of chylomicrons and treated with BFA, were fixed with methanol and immunostained for ApoB (red) and Sec31, TANGO1, or ERGIC-53 (green). Boron-dipyrromethene (BODIPY) was used to visualize lipid droplets (blue). DAPI is shown in gray. Bars, 5 µm. (C) Scheme depicting the methodology used to differentiate and induce chylomicron secretion in Caco-2 while inhibiting autophagy and inhibiting ER export with BFA. (D) Differentiated parental, TANGO1-KO, or TALI-KO Caco-2 cells, induced for secretion of chylomicrons and treated with BFA or with wortmannin and BFA, were fixed with methanol and immunostained for ApoB (red) and Sec31 (green). BODIPY was used to visualize lipid droplets (blue). DAPI is shown in gray. Bars, 5 µm. (E) Colocalization quantifications were calculated by Manders correlation coefficient by measuring the overlap between the green and the red channels. Error bars: SEM; ***, $P < 0.001$; ≥100 cells per experiment; $n = 3$. (F) The number of ApoB crescents was counted by immunofluorescence microscopy, and counts were divided by the total number of cells per field of view. Error bars: SEM; ***, $P < 0.001$; N.S, not statistically significant; ≥100 cells per experiment; $n = 3$.

increases the pool of the inner-coat proteins Sec23/Sec24 (Saito et al., 2014). On the other hand, KLHL12 is reported to ubiquitinate Sec31 and is suggested to increase the size of the outer layer of COPII coats (Jin et al., 2012). Undoubtedly, the mechanism of procollagen export from the ER is likely more complicated, but identification of these players provides a means to dissect this process of fundamental importance (Malhotra and Erlmann, 2015; Malhotra et al., 2015). Our new data in Caco-2 cells reveal that TANGO1 is required for the export of procollagen XII from the ER (Fig. 5). This, in addition to the published data on the role of TANGO1 in the secretion of many other collagens in mice (Wilson et al., 2011), suggests that TANGO1 has a more general role in the export of procollagens from the ER, and thus not a restricted role in procollagen VII export, as we had previously stated (Nogueira et al., 2014).

TALI and TANGO1 are required for the export of ApoB-containing lipid particles from the ER

Upon differentiation into enterocytes, Caco-2 cells secrete chylomicrons and the hepatocyte cell line HepG2 secretes VLDLs, in a TANGO1- and TALI-dependent manner (Figs. 2, 3, and 4). Interestingly, unlike TANGO1, deletion of TALI had no obvious effect on collagen XII secretion (Fig. 5). A straightforward finding would have been that TANGO1 is involved in the export of procollagens and TALI takes charge of the export of bulky lipid particles. However, our data show that deletion of TANGO1 affected secretion of ApoB by 44% compared with parental cells. Knockout of TALI, on the other hand, reduced ApoB secretion by 82% (Fig. 2, E and F). This suggests that both TANGO1 and TALI play a role in the export of bulky chylomicrons from the

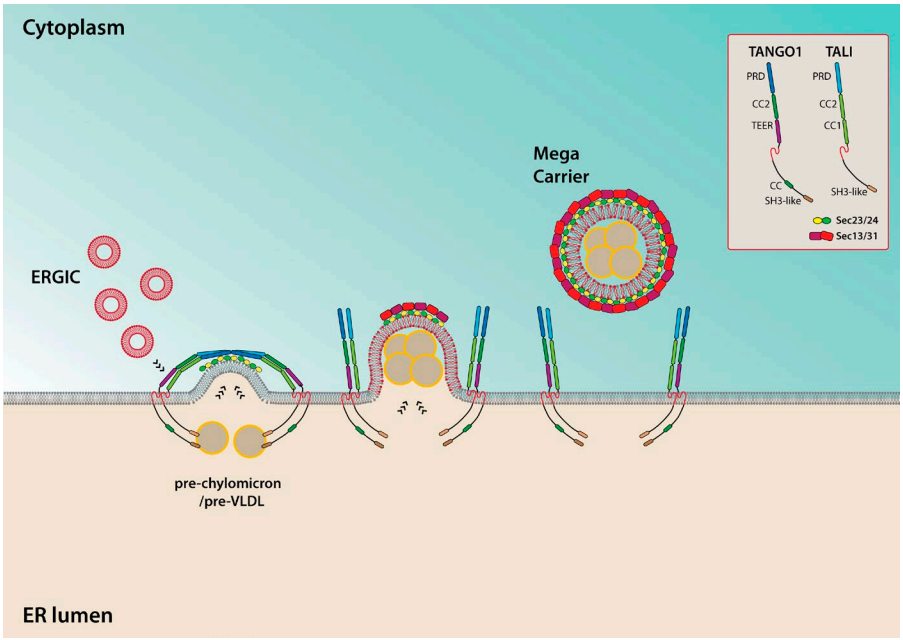

Figure 8. **Model for the export of pre-chylomicrons/VLDLs from the ER.** TANGO1 and TALI interact with ApoB directly or through an adaptor protein in the lumen of the ER to bring pre-chylomicrons/VLDLs to ER exit sites. On the cytoplasmic side, the TEER domain of TANGO1 recruits ERGIC membranes that fuse to the ER exit site that is now enriched in pre-chylomicrons/VLDLs. Binding of the proline-rich domain (PRD) of TANGO1 and TALI on the cytoplasmic side to Sec23/24 prevents Sec13/31 recruitment, allowing continuous fusion of ERGIC membranes that result in the growth of a mega-bud that is packed with pre-chylomicrons/VLDLs. Fission is triggered, and a mega carrier, big enough to accommodate bulky pre-chylomicrons/VLDLs, is released from the ER.

ER. But why is the effect of TALI KO so severe on chylomicron export compared with the KO of TANGO1? One possibility is that an adaptor protein necessary for the export of chylomicrons has a weak affinity for TALI, which is potentiated by binding to TANGO1. In cells lacking TANGO1, this presumed adaptor can still interact with TALI, albeit weakly, which affects the overall efficiency of chylomicron export. Both TANGO1 and TALI interact with each other and with ApoB, and BFA treatment blocks export of cargoes from the ER at exit sites (Figs. 6 and 7, A and B). Interestingly, in the absence of TANGO1 or TALI, ApoB did not accumulate at ER exit sites upon treatment with BFA, indicating that without either TANGO1 or TALI, ApoB-containing bulky lipid particles do not reach the ER sites for export (Fig. 7, D–F). These data suggest that TANGO1 and TALI might form a receptor complex for bulky pre-chylomicrons and pre-VLDLs at ER exit sites. Altogether, our data indicate that TANGO1 and TALI both participate in the binding and concentration of ApoB-containing lipid particles for their subsequent export from the ER.

We have found that knockout of TANGO1 and TALI resulted in intracellular accumulation of ApoB that colocalized with autolysosomes, because they were positive for LAMP1, a lysosomal marker, and LC3, an autophagosomal marker (Fig. 3). This indicates the existence of a mechanism to ensure intracellular homeostasis of these lipoprotein particles. A defect in their export probably triggers a signal for clearance by autophagy of the ER domains where these lipid particles accumulate. We expect that the same applies to other bulky cargoes, such as collagens, when they accumulate in the ER. The balance between synthesis of abundant and bulky cargoes and the decision for their export or degradation is an additional interesting challenge.

Dissecting the mechanism for the export of bulky pre-chylomicrons and pre-VLDLs from the ER

We have shown that without the SH3-like domain, TANGO1 is incapable of binding to procollagen VII (Saito et al., 2009). Interestingly, it has been shown that mice expressing TALI carrying a mutation in its SH3-like domain exhibited lower levels of cholesterol and triglycerides in the blood (Pitman et al., 2011). This observation suggests that the SH3-like domain of TALI is involved in the capture of pre-chylomicrons and pre-VLDLs in the lumen of the ER. But there is no obvious sequence or structural similarity between collagens and ApoB. How can the SH3-like domains of TANGO1 and TALI interact with such diverse cargoes? One possibility is that the SH3-like domain binds a common linker or chaperone for these two distinct classes of cargoes and that the specificity is provided by the other parts of lumenal TANGO1 or TALI. TANGO1 contains a coiled-coil domain in addition to the SH3-like domain in the lumen of the ER. TALI lacks this coiled-coil domain. This difference might affect the ability to control their interaction with specific clients in the ER lumen. Identification of the binding partners of TANGO1 and TALI in the ER will help in understanding the functional significance of their individual domains in the overall process by which specific cargoes are collected and concentrated for subsequent export. But overall, why cells use both TANGO1 and TALI for the export of bulky lipid particles remains an interesting challenge. Could this be caused by the difference in the shape of the cargoes: a spherical lipid particle versus a long rod-like collagen trimer? All these suggestions are difficult to test experimentally at present but provide working hypotheses for future investigations into the mechanism by which cargoes are selected and exported by these cargo receptors at the ER.

Based on our findings, we suggest that TANGO1 and TALI work together to collect ApoB-containing lipid particles in the lumen of the ER. TANGO1 is known to bind cTAGE5, and because the cytoplasmic domain of TALI is in fact cTAGE5, it is not a surprise that TALI coimmunoprecipitates with TANGO1 (Fig. 6 B). So, we propose that cTAGE5/TALI recruits Sec12 and subsequently Sec23/Sec24 to the ER exit site and, in contrast, the TEER domain of TANGO1 recruits ERGIC membranes to the ER exit site enriched in ApoB-containing lipid particles (Fig. 8). In other words, the overall mechanism to generate an export carrier for pre-chylomicrons and pre-VLDLs by TALI and TANGO1 is the same as that used for the generation of procollagen-containing export carriers by TANGO1 alone.

In conclusion, our data suggest that TANGO1 and TALI are the receptors in the ER for export of bulky pre-chylomicrons and pre-VLDLs. They therefore emerge as key players in the overall process by which cells export bulky cargoes from the ER. We show here that a defect in capture of these lipoproteins and their subsequent export from the ER leads to defective secretion. In a physiological context, such a defect would lead to dramatic changes in the levels of circulating cholesterol and triglycerides in the blood.

Materials and methods

RT-PCR and DNA constructs

To determine the sequence of the fusion of MIA2/cTAGE5 gene products (TALI), lysed Caco-2 cells and their total RNA were extracted with the RNeasy extraction kit (Qiagen). cDNA was synthesized by RT-PCR with Superscript III (Invitrogen). Primers for the N terminus of *MIA2* and the C terminus of *cTAGE5* were used. We then amplified the same fragment to clone it into the lentiviral vector PLJM1 with an EGFP tag on the C terminus. pLJM1-EGFP was a gift from D. Sabatini, Whitehead Institute, Cambridge, MA, (plasmid 19319; Addgene). To determine the differential expression patterns of TANGO1, TALI, and ApoB in the different human tissues, we used the Human MTC panel I and II (Clontech Laboratories) of first-strand cDNAs for amplification. To measure the expression of ApoB and MTP, differentiated Caco-2 cells were lysed, total RNA was extracted, and cDNA was synthesized as described earlier. Real-time PCR was performed with Light Cycler 480 SYBR Green I Master (Roche) according to the manufacturer's instructions. SnapGene software (GSL Biotech) was used for molecular cloning design.

Cell culture

Caco-2 and HepG2 cells were grown at 37°C with 5% CO_2 in complete DMEM with 20% and 10% FBS, respectively. For lentiviral infection of TALI-EGFP into Caco-2 cells, lentiviral particles were produced by cotransfecting HEK293 cells with a third-generation packaging vector pool and pJLM1-TALI-EGFP using TransIT-293 (Mirus). 72 h after transfection, the viral supernatant was harvested, filtered, and directly added to Caco-2 cells. In HepG2 cells, TALI-EGFP was transfected with Lipofectamine 3000 (Thermo Fisher Scientific) according to the manufacturer's protocols.

Generation of TANGO1 and TALI KO cell lines by CRISPR

To generate Caco-2 and HepG2 cell lines in which TANGO1 or TALI expression was abolished, we performed genome editing with the CRISPR/Cas9 system. We obtained a pool of three plasmids each containing a 20-nt gRNA sequence designed to target double-strand breaks in the TANGO1 or TALI coding sequences (in both cases corresponding to the sequence encoding for the lumenal portion of the protein) and the pSpCas9 ribonuclease (sc-403994 and sc-418205; Santa Cruz Biotechnology, Inc.). In addition, plasmids contained an EGFP coding sequence or a puromycin resistance sequence to allow for positive selection of transfected cells. Both Caco-2 and HepG2 cells were transfected with 1 µg of pooled plasmid using Lipofectamine 3000 transfection (Life Technologies). For Caco-2 cells, 96 h after transfection, EGFP-positive cells were isolated by FACS, and single cells were collected in 96-well plates. For HepG2 cells, 72 h after transfection, puromycin was added to the cells at a concentration of 1 µg/ml, and selection occurred for 10 d. After expansion to six-well format, Caco-2 and HepG2 cells were collected and protein lysates were prepared to assess TANGO1 or TALI presence by Western blotting.

Lipid particle-secretion assays

Caco-2 cells were grown for 21 d to differentiate, with changes to fresh medium every 3 d. HepG2 cells were grown for 5–10 d with changes to fresh medium every 3 d. To induce chylomicron/VLDL secretion, FCS-free medium with oleic acid (1.5 mM; Sigma-Aldrich) solubilized in fatty acid–free BSA (Sigma-Aldrich) was added to the cells for 5 h. For the autophagy-inhibition experiments, wortmannin (Calbiochem) was added at a concentration of 1 µM for 16 h and then increased to 2 µM during the 5-h induction period. To block ER export, BFA (Sigma-Aldrich) was added to the cells at a concentration of 10 µg/ml during the 5-h period of induction. After this, cells were either processed for immunofluorescence microscopy or the media were centrifuged at low speed to remove any cells or cellular debris. For TCA precipitation, 1/100 of 2% deoxycholate was mixed with the medium and left for 30 min at 4°C, then 1/10 of TCA was mixed and left overnight at 4°C. The mix was centrifugated for 15 min at 4°C at 14,000 rpm, and the pellets were recovered with Laemmli SDS sample buffer. For cell lysis, the cells were washed with PBS, lysed, and centrifuged at 14,000 rpm for 15 min at 4°C. The supernatants were boiled for 5 min with Laemmli SDS sample buffer. Media and cell lysate were subjected to SDS-PAGE (6% or 10% acrylamide) and Western blotting with the relevant antibodies. ImageJ (National Institutes of Health) was used for densitometric quantification of Western blots.

Silver staining

A 6% SDS-PAGE acrylamide gel was fixed for 1 h with 50% methanol and 10% acetic acid at RT. After washes with water, sodium thiosulfate (0.05 g/l) was added to the gel for 90 s. After washing, silver nitrate (0.002 g/ml) was added for 25 min. The gel was washed and developed with 0.03 g/ml sodium carbonate in 2% sodium thiosulfate/0.02% formaldehyde. After washing and removing the developing solution, a solution of 6% acetic acid was added for 10 min and then replaced by water.

Mass spectrometry

Peptides were removed from silver-stained gel bands with iodoacetamide precipitation. After digestion with trypsin, peptides were acidified and desalted before LC-MS/MS analysis. 45% of each sample was analyzed using a LTQ-Orbitrap XL mass spectrometer (Thermo Fisher Scientific) coupled to an EasyLC (Thermo Fisher Scientific). All data were acquired with Xcalibur software. Proteome Discoverer software suite (Thermo Fisher Scientific) and the Mascot search engine (Matrix Science) were used for peptide identification and quantification. The data were searched against the human SwissProt database. Resulting data files were filtered for ion score 20.

Collagen-secretion assays

The medium of differentiated Caco-2 cells was replaced with a FCS-free fresh medium containing 1 mM ascorbic acid for 20 h to allow for collagen secretion. The media were centrifuged at low speed to remove any cells or cellular debris, and the supernatant was boiled for 5 min with Laemmli SDS sample buffer. For cell lysis, the cells were washed with PBS, lysed, and centrifuged at 14,000 rpm for 15 min at 4°C. The supernatants were boiled for 5 min with Laemmli SDS sample buffer. Media and cell lysate were subjected to SDS-PAGE (6% acrylamide) and Western blotting with collagen XII and α-tubulin antibodies.

Immunofluorescence microscopy

Cells grown on coverslips were fixed with cold methanol for 10 min at −20°C and incubated with blocking reagent (Roche) for 30 min at RT. Primary antibodies were diluted in blocking reagent and incubated overnight at 4°C. Secondary antibodies conjugated with Alexa Fluor 488, 555, 594, or 647 (Invitrogen) were diluted in blocking reagent and

incubated for 1 h at RT. Images were taken with a TCS SPE or TCS SP5 confocal microscope (Leica) with a 63× objective. Two-channel colocalization analysis was performed using ImageJ, and the Manders correlation coefficient was calculated using the plugin JaCop (Bolte and Cordelières, 2006).

Coimmunoprecipitation

HepG2 cells induced with oleic acid–BSA for 5 h (see earlier) were lysed with Hepes-CHAPS lysis buffer (2% CHAPS in 50 mM Hepes and 200 mM NaCl, pH 7.5; Roche) containing a mixture of protease inhibitors (Roche) for 30 min on ice. The lysates were incubated for 16 h with rotation at 4°C without antibody or with anti-TANGO1, anti-cTAGE5, or anti-MIA2 antibodies. Protein A–Sepharose beads (GE Healthcare) were added to the cell lysates and incubated with rotation for 3 h at 4°C. Immunoprecipitates were washed four times with wash buffer (0.5% CHAPS in Hepes buffer), resuspended in TE buffer (10 mM Tris-HCl, pH 6.8, and 1 mM EDTA), and heated to 95°C for 5 min. Laemmli SDS sample buffer was added, and the samples were heated for another 5 min at 95°C. The samples were subjected to SDS-PAGE (6%) and Western blotting with the indicated antibodies.

Antibodies

Antibodies used in Western blotting and immunofluorescence microscopy were as follows: EGFP (Roche); TANGO1 and α-tubulin (Sigma-Aldrich); cTAGE5 (Atlas Antibodies); apolipoprotein B (Tebubio); apolipoprotein E, GRP78/BIP, PDI, and LAMP1 (Abcam); Sec31A (BD); calreticulin (Novus Biologicals); and LC3, ERGIC-53, and collagen XII (Santa Cruz). For the coimmunoprecipitation experiments, besides the anti-TANGO1 and anti-cTAGE5 antibodies, an anti-MIA2 antibody (Antigenix America) was used.

Statistical analysis

Results shown are mean ± SEM. Statistical testing was performed using Student's *t* test (continuous data, two groups) always before normalization was performed. For immunofluorescence microscopy analysis, the number of cells was always greater than 100. The number of experiments was more than three for each quantification.

Acknowledgments

We thank members of the Malhotra laboratory for valuable discussions and feedback in manuscript preparation, especially Dr. Nathalie Brouwers for helping in the generation of the TALI-CrispR cells. We also thank Christine Panagiotidis for invaluable help in the illustration of the model. All confocal imaging was performed at the Centre for Genomic Regulation Advanced Light Microscopy Unit.

We acknowledge support of the Ministerio de Economía y Competitividad, "Centro de Excelencia Severo Ochoa 2013-2017," SEV-2012-0208. The research leading to these results has received funding from the European Union Seventh Framework Programme (FP7/2007-2013) under grant agreement 625149 to A.J.M. Santos and European Research Council grant agreement 268692 to V. Malhotra. This work reflects only the author's views, and the community is not liable for any use that may be made of the information contained therein. V. Malhotra is an Institució Catalana de Recerca i Estudis Avançats professor at the Center for Genomic Regulation, and the work in his laboratory is funded by grants from Ministerio de Economía y Competitividad's Plan Nacional (ref. BFU2013-44188-P) and Consolider (CSD2009-00016).

The authors declare no competing financial interests.

Submitted: 21 March 2016
Accepted: 14 April 2016

References

Barlowe, C., and R. Schekman. 1993. SEC12 encodes a guanine-nucleotide-exchange factor essential for transport vesicle budding from the ER. *Nature.* 365:347–349. http://dx.doi.org/10.1038/365347a0

Bernales, S., S. Schuck, and P. Walter. 2007. ER-phagy: Selective autophagy of the endoplasmic reticulum. *Autophagy.* 3:285–287. http://dx.doi.org/10.4161/auto.3930

Blommaart, E.F., U. Krause, J.P. Schellens, H. Vreeling-Sindelárová, and A.J. Meijer. 1997. The phosphatidylinositol 3-kinase inhibitors wortmannin and LY294002 inhibit autophagy in isolated rat hepatocytes. *Eur. J. Biochem.* 243:240–246. http://dx.doi.org/10.1111/j.1432-1033.1997.0240a.x

Bolte, S., and F.P. Cordelières. 2006. A guided tour into subcellular colocalization analysis in light microscopy. *J. Microsc.* 224:213–232. http://dx.doi.org/10.1111/j.1365-2818.2006.01706.x

Brodsky, J.L., and E.A. Fisher. 2008. The many intersecting pathways underlying apolipoprotein B secretion and degradation. *Trends Endocrinol. Metab.* 19:254–259. http://dx.doi.org/10.1016/j.tem.2008.07.002

Cong, L., F.A. Ran, D. Cox, S. Lin, R. Barretto, N. Habib, P.D. Hsu, X. Wu, W. Jiang, L.A. Marraffini, and F. Zhang. 2013. Multiplex genome engineering using CRISPR/Cas systems. *Science.* 339:819–823. http://dx.doi.org/10.1126/science.1231143

Fromme, J.C., and R. Schekman. 2005. COPII-coated vesicles: Flexible enough for large cargo? *Curr. Opin. Cell Biol.* 17:345–352. http://dx.doi.org/10.1016/j.ceb.2005.06.004

García-Bermúdez, M., R. López-Mejías, C. González-Juanatey, A. Corrales, S. Castañeda, J.A. Miranda-Filloy, C. Gómez-Vaquero, B. Fernández-Gutiérrez, A. Balsa, D. Pascual-Salcedo, et al. 2012. Association study of MIA3 rs17465637 polymorphism with cardiovascular disease in rheumatoid arthritis patients. *DNA Cell Biol.* 31:1412–1417. http://dx.doi.org/10.1089/dna.2012.1672

Iqbal, J., and M.M. Hussain. 2009. Intestinal lipid absorption. *Am. J. Physiol. Endocrinol. Metab.* 296:E1183–E1194. http://dx.doi.org/10.1152/ajpendo.90899.2008

Jammart, B., M. Michelet, E.I. Pécheur, R. Parent, B. Bartosch, F. Zoulim, and D. Durantel. 2013. Very-low-density lipoprotein (VLDL)-producing and hepatitis C virus-replicating HepG2 cells secrete no more lipoviroparticles than VLDL-deficient Huh7.5 cells. *J. Virol.* 87:5065–5080. http://dx.doi.org/10.1128/JVI.01405-12

Jiang, Z.G., Y. Liu, M.M. Hussain, D. Atkinson, and C.J. McKnight. 2008. Reconstituting initial events during the assembly of apolipoprotein B-containing lipoproteins in a cell-free system. *J. Mol. Biol.* 383:1181–1194. http://dx.doi.org/10.1016/j.jmb.2008.09.006

Jin, L., K.B. Pahuja, K.E. Wickliffe, A. Gorur, C. Baumgärtel, R. Schekman, and M. Rape. 2012. Ubiquitin-dependent regulation of COPII coat size and function. *Nature.* 482:495–500. http://dx.doi.org/10.1038/nature10822

Khaminets, A., T. Heinrich, M. Mari, P. Grumati, A.K. Huebner, M. Akutsu, L. Liebmann, A. Stolz, S. Nietzsche, N. Koch, et al. 2015. Regulation of endoplasmic reticulum turnover by selective autophagy. *Nature.* 522:354–358. http://dx.doi.org/10.1038/nature14498

Korolchuk, V.I., S. Saiki, M. Lichtenberg, F.H. Siddiqi, E.A. Roberts, S. Imarisio, L. Jahreiss, S. Sarkar, M. Futter, F.M. Menzies, et al. 2011. Lysosomal positioning coordinates cellular nutrient responses. *Nat. Cell Biol.* 13:453–460. http://dx.doi.org/10.1038/ncb2204

Kuehn, M.J., J.M. Herrmann, and R. Schekman. 1998. COPII-cargo interactions direct protein sorting into ER-derived transport vesicles. *Nature.* 391:187–190. http://dx.doi.org/10.1038/34438

Li, X., Y. Huang, D. Yin, D. Wang, C. Xu, F. Wang, Q. Yang, X. Wang, S. Li, S. Chen, et al. 2013. Meta-analysis identifies robust association between SNP rs17465637 in MIA3 on chromosome 1q41 and coronary artery disease. *Atherosclerosis.* 231:136–140. http://dx.doi.org/10.1016/j.atherosclerosis.2013.08.031

Lord, C., S. Ferro-Novick, and E.A. Miller. 2013. The highly conserved COPII coat complex sorts cargo from the endoplasmic reticulum and targets it to the golgi. *Cold Spring Harb. Perspect. Biol.* 5:5. http://dx.doi.org/10.1101/cshperspect.a013367

Malhotra, V., and P. Erlmann. 2011. Protein export at the ER: Loading big collagens into COPII carriers. *EMBO J.* 30:3475–3480. http://dx.doi.org/10.1038/emboj.2011.255

Malhotra, V., and P. Erlmann. 2015. The pathway of collagen secretion. *Annu. Rev. Cell Dev. Biol.* 31:109–124. http://dx.doi.org/10.1146/annurev-cellbio-100913-013002

Malhotra, V., P. Erlmann, and C. Nogueira. 2015. Procollagen export from the endoplasmic reticulum. *Biochem. Soc. Trans.* 43:104–107. http://dx.doi.org/10.1042/BST20140286

Mali, P., L. Yang, K.M. Esvelt, J. Aach, M. Guell, J.E. DiCarlo, J.E. Norville, and G.M. Church. 2013. RNA-guided human genome engineering via Cas9. *Science.* 339:823–826. http://dx.doi.org/10.1126/science.1232033

Matsuoka, K., L. Orci, M. Amherdt, S.Y. Bednarek, S. Hamamoto, R. Schekman, and T. Yeung. 1998. COPII-coated vesicle formation reconstituted with purified coat proteins and chemically defined liposomes. *Cell.* 93:263–275. http://dx.doi.org/10.1016/S0092-8674(00)81577-9

Meex, S.J., U. Andreo, J.D. Sparks, and E.A. Fisher. 2011. Huh-7 or HepG2 cells: Which is the better model for studying human apolipoprotein-B100 assembly and secretion? *J. Lipid Res.* 52:152–158. http://dx.doi.org/10.1194/jlr.D008888

Nakajima, K., T. Nagamine, M.Q. Fujita, M. Ai, A. Tanaka, and E. Schaefer. 2014. Apolipoprotein B-48: A unique marker of chylomicron metabolism. *Adv. Clin. Chem.* 64:117–177. http://dx.doi.org/10.1016/B978-0-12-800263-6.00003-3

Nakano, T., K. Nakajima, M. Niimi, M.Q. Fujita, Y. Nakajima, S. Takeichi, M. Kinoshita, T. Matsushima, T. Teramoto, and A. Tanaka. 2008. Detection of apolipoproteins B-48 and B-100 carrying particles in lipoprotein fractions extracted from human aortic atherosclerotic plaques in sudden cardiac death cases. *Clin. Chim. Acta.* 390:38–43. http://dx.doi.org/10.1016/j.cca.2007.12.012

Nakańo, A., and M. Muramatsu. 1989. A novel GTP-binding protein, Sar1p, is involved in transport from the endoplasmic reticulum to the Golgi apparatus. *J. Cell Biol.* 109:2677–2691. http://dx.doi.org/10.1083/jcb.109.6.2677

Nauli, A.M., Y. Sun, J.D. Whittimore, S. Atyia, G. Krishnaswamy, and S.M. Nauli. 2014. Chylomicrons produced by Caco-2 cells contained ApoB-48 with diameter of 80-200 nm. *Physiol. Rep.* 2:2. http://dx.doi.org/10.14814/phy2.12018

Nogueira, C., P. Erlmann, J. Villeneuve, A.J. Santos, E. Martínez-Alonso, J.A. Martínez-Menárguez, and V. Malhotra. 2014. SLY1 and Syntaxin 18 specify a distinct pathway for procollagen VII export from the endoplasmic reticulum. *eLife.* 3:e02784. http://dx.doi.org/10.7554/eLife.02784

Ohsaki, Y., J. Cheng, A. Fujita, T. Tokumoto, and T. Fujimoto. 2006. Cytoplasmic lipid droplets are sites of convergence of proteasomal and autophagic degradation of apolipoprotein B. *Mol. Biol. Cell.* 17:2674–2683. http://dx.doi.org/10.1091/mbc.E05-07-0659

Ohsaki, Y., J. Cheng, M. Suzuki, A. Fujita, and T. Fujimoto. 2008. Lipid droplets are arrested in the ER membrane by tight binding of lipidated apolipoprotein B-100. *J. Cell Sci.* 121:2415–2422. http://dx.doi.org/10.1242/jcs.025452

Ohsaki, Y., J. Cheng, K. Yamairi, X. Pan, M.M. Hussain, and T. Fujimoto. 2013. Inhibition of ADP-ribosylation suppresses aberrant accumulation of lipidated apolipoprotein B in the endoplasmic reticulum. *FEBS Lett.* 587:3696–3702. http://dx.doi.org/10.1016/j.febslet.2013.09.036

Olofsson, S.O., and J. Borén. 2012. Apolipoprotein B secretory regulation by degradation. *Arterioscler. Thromb. Vasc. Biol.* 32:1334–1338. http://dx.doi.org/10.1161/ATVBAHA.112.251116

Pal, S., K. Semorine, G.F. Watts, and J. Mamo. 2003. Identification of lipoproteins of intestinal origin in human atherosclerotic plaque. *Clin. Chem. Lab. Med.* 41:792–795. http://dx.doi.org/10.1515/CCLM.2003.120

Pitman, J.L., D.J. Bonnet, L.K. Curtiss, and N. Gekakis. 2011. Reduced cholesterol and triglycerides in mice with a mutation in Mia2, a liver protein that localizes to ER exit sites. *J. Lipid Res.* 52:1775–1786. http://dx.doi.org/10.1194/jlr.M017277

Plump, A.S., J.D. Smith, T. Hayek, K. Aalto-Setälä, A. Walsh, J.G. Verstuyft, E.M. Rubin, and J.L. Breslow. 1992. Severe hypercholesterolemia and atherosclerosis in apolipoprotein E-deficient mice created by homologous recombination in ES cells. *Cell.* 71:343–353. http://dx.doi.org/10.1016/0092-8674(92)90362-G

Proctor, S.D., and J.C. Mamo. 2003. Intimal retention of cholesterol derived from apolipoprotein B100- and apolipoprotein B48-containing lipoproteins in carotid arteries of Watanabe heritable hyperlipidemic rabbits. *Arterioscler. Thromb. Vasc. Biol.* 23:1595–1600. http://dx.doi.org/10.1161/01.ATV.0000084638.14534.0A

Roder, C., V. Peters, H. Kasuya, T. Nishizawa, Y. Takehara, D. Berg, C. Schulte, N. Khan, M. Tatagiba, and B. Krischek. 2011. Common genetic polymorphisms in moyamoya and atherosclerotic disease in Europeans. *Childs Nerv. Syst.* 27:245–252. http://dx.doi.org/10.1007/s00381-010-1241-8

Ruf, H., and B.J. Gould. 1999. Size distributions of chylomicrons from human lymph from dynamic light scattering measurements. *Eur. Biophys. J.* 28:1–11. http://dx.doi.org/10.1007/s002490050178

Saito, K., M. Chen, F. Bard, S. Chen, H. Zhou, D. Woodley, R. Polischuk, R. Schekman, and V. Malhotra. 2009. TANGO1 facilitates cargo loading at endoplasmic reticulum exit sites. *Cell.* 136:891–902. http://dx.doi.org/10.1016/j.cell.2008.12.025

Saito, K., K. Yamashiro, Y. Ichikawa, P. Erlmann, K. Kontani, V. Malhotra, and T. Katada. 2011. cTAGE5 mediates collagen secretion through interaction with TANGO1 at endoplasmic reticulum exit sites. *Mol. Biol. Cell.* 22:2301–2308. http://dx.doi.org/10.1091/mbc.E11-02-0143

Saito, K., K. Yamashiro, N. Shimazu, T. Tanabe, K. Kontani, and T. Katada. 2014. Concentration of Sec12 at ER exit sites via interaction with cTAGE5 is required for collagen export. *J. Cell Biol.* 206:751–762. http://dx.doi.org/10.1083/jcb.201312062

Santos, A.J., I. Raote, M. Scarpa, N. Brouwers, and V. Malhotra. 2015. TANGO1 recruits ERGIC membranes to the endoplasmic reticulum for procollagen export. *eLife.* 4:4. http://dx.doi.org/10.7554/eLife.10982

Siddiqi, S.A. 2008. VLDL exits from the endoplasmic reticulum in a specialized vesicle, the VLDL transport vesicle, in rat primary hepatocytes. *Biochem. J.* 413:333–342. http://dx.doi.org/10.1042/BJ20071469

Siddiqi, S.A., F.S. Gorelick, J.T. Mahan, and C.M. Mansbach II. 2003. COPII proteins are required for Golgi fusion but not for endoplasmic reticulum budding of the pre-chylomicron transport vesicle. *J. Cell Sci.* 116:415–427. http://dx.doi.org/10.1242/jcs.00215

Stagg, S.M., C. Gürkan, D.M. Fowler, P. LaPointe, T.R. Foss, C.S. Potter, B. Carragher, and W.E. Balch. 2006. Structure of the Sec13/31 COPII coat cage. *Nature.* 439:234–238. http://dx.doi.org/10.1038/nature04339

Tomkin, G.H., and D. Owens. 2012. The chylomicron: Relationship to atherosclerosis. *Int. J. Vasc. Med.* 2012:784536. http://dx.doi.org/10.1155/2012/784536

van Greevenbroek, M.M., D.W. Erkelens, and T.W. de Bruin. 2000. Caco-2 cells secrete two independent classes of lipoproteins with distinct density: Effect of the ratio of unsaturated to saturated fatty acid. *Atherosclerosis.* 149:25–31. http://dx.doi.org/10.1016/S0021-9150(99)00289-0

Venditti, R., T. Scanu, M. Santoro, G. Di Tullio, A. Spaar, R. Gaibisso, G.V. Beznoussenko, A.A. Mironov, A. Mironov Jr., L. Zelante, et al. 2012. Sedlin controls the ER export of procollagen by regulating the Sar1 cycle. *Science.* 337:1668–1672. http://dx.doi.org/10.1126/science.1224947

Wilson, D.G., K. Phamluong, L. Li, M. Sun, T.C. Cao, P.S. Liu, Z. Modrusan, W.N. Sandoval, L. Rangell, R.A. Carano, et al. 2011. Global defects in collagen secretion in a Mia3/TANGO1 knockout mouse. *J. Cell Biol.* 193:935–951. http://dx.doi.org/10.1083/jcb.201007162

Xie, Z., and D.J. Klionsky. 2007. Autophagosome formation: Core machinery and adaptations. *Nat. Cell Biol.* 9:1102–1109. http://dx.doi.org/10.1038/ncb1007-1102

Yates, A., W. Akanni, M.R. Amode, D. Barrell, K. Billis, D. Carvalho-Silva, C. Cummins, P. Clapham, S. Fitzgerald, L. Gil, et al. 2016. Ensembl 2016. *Nucleic Acids Res.* 44(D1):D710–D716. http://dx.doi.org/10.1093/nar/gkv1157

Zhang, S.H., R.L. Reddick, J.A. Piedrahita, and N. Maeda. 1992. Spontaneous hypercholesterolemia and arterial lesions in mice lacking apolipoprotein E. *Science.* 258:468–471. http://dx.doi.org/10.1126/science.1411543

Zheng, C., S.J. Murdoch, J.D. Brunzell, and F.M. Sacks. 2006. Lipoprotein lipase bound to apolipoprotein B lipoproteins accelerates clearance of postprandial lipoproteins in humans. *Arterioscler. Thromb. Vasc. Biol.* 26:891–896. http://dx.doi.org/10.1161/01.ATV.0000203512.01007.3d